Ultrasound in Med. & Biol., Vol. 28, No. 5, pp. 561–569, 2002

0301-5629/02/$–see front matter

PII: S0301-5629(02)00496-9

● *Original Contribution*

ASSESSMENT OF NORMAL AND ISCHAEMIC MYOCARDIUM BY QUANTITATIVE M-MODE TISSUE DOPPLER IMAGING

MANUEL DESCO,* MARÍA J. LEDESMA-CARBAYO,‡ ESTHER PÉREZ,† ANDRÉS SANTOS,‡ JOSÉ C. ANTORANZ,§ NORBERTO MALPICA,‡§ PEDRO MARCOS-ALBERCA† and MIGUEL A. GARCÍA-FERNÁNDEZ†

*Medicina y Cirugía Experimental and †Laboratorio de Ecocardiografia, Departamento de Cardiologia, Hospital General Universitario Gregorio Marañón, Madrid, Spain; ‡Departamento de Ingeniería Electrónica, ETSI Telecomunicación, Universidad Politécnica de Madrid, Madrid, Spain; and §Departamento de Física Matemática y Fluidos, Universidad Nacional de Educación a Distancia, Madrid, Spain

(*Received* 28 *August* 2001; *in final form* 6 *February* 2002)

Abstract—This paper presents a methodology and a software package developed to quantify M-mode tissue Doppler imaging (TDI), defining a number of quantitative parameters drawn from velocity and gradient curves obtained after segmenting the myocardial wall into anatomical layers. The independent clinical predictive value of these parameters to detect motion abnormalities in the presence of ischaemia was evaluated in a comparative study between a group of 17 healthy volunteers and 18 ischaemic patients. Factor analysis and stepwise logistic regression were used to assess the independent predictive value of these parameters in detecting abnormal contractility of the basal posterior segment. The statistical analysis performed has proved that any single parameter related to the gradient intensity, particularly the maximum gradient at the moment of the "e" wave, provides meaningful clinical information, achieving a rate of correct classification of 79.1% on the same data set used for the analysis. Adding additional parameters does not improve the diagnostic performance. Further testing with different settings (stress studies, other pathologies or segments) is warranted. (E-mail: desco@mce.hggm.es) **© 2002 World Federation for Ultrasound in Medicine & Biology.**

Key Words: **Echocardiography, Tissue Doppler imaging, Quantification, Ischaemic heart disease, M-mode, Diastole.**

INTRODUCTION

Tissue Doppler imaging (TDI) is a relatively recent non-invasive ultrasound (US) technique that allows the measurement of velocities at any point in the ventricular wall during the cardiac cycle. It produces velocity maps, displayed as a colour overlay superimposed on the grey-scale 2-D or M-mode image (Desco and Antoranz 1997; Palka et al. 1995; Sutherland et al. 1994). M-mode or 2-D tissue Doppler images also allow for the analysis of regional left ventricular wall motion dynamics (García-Fernández et al. 1997).

Several studies have been carried out to determine normal values of myocardial velocities and to show its sensitivity to detect wall motion abnormalities in several pathologies (Derumeaux et al. 1997; Desco et al. 1996; Donovan et al. 1995; Miyatake et al. 1995; Yamazaki et al. 1994). Regional myocardial function has been largely studied with conventional echocardiography by the analysis of the endocardial border displacement (Jacob et al. 1999; Malassiotis and Strintzis 1999). However, the ability of TDI to provide information on the exact timing and magnitude of intramural wall velocities makes it a promising tool for the diagnosis of myocardial ischaemia (Derumeaux et al. 1998; Garcia-Fernandez et al. 1999; Garot et al. 2000; Gorcsan et al. 1997). Preliminary studies on M-mode TDI images have reported a nonuniform distribution of intramyocardial velocities in the presence of ischaemia, as well as different temporal evolution of diastolic velocities (Derumeaux et al. 2000; Marcos-Alberca et al. 2001). The study of the intramural myocardial velocity gradient obtained from TDI M-mode images has been proposed to assess myocardial contractility defects in ischaemic segments (Fleming et al. 1994b; Pellerin et al. 1999).

Address correspondence to: Manuel Desco, Ph.D., Medicina y Cirugía Experimental Hospital G. U. Gregorio Marañón, C/Dr. Esquerdo 46, E-28007 Madrid, Spain. E-mail: desco@mce.hggm.es

However, clinical interpretation of the results is not straightforward. Regional quantitative analysis is required to detect subtle intramyocardial motion abnormalities that cannot be evaluated by visual analysis. Although, today, commercial scanners include analysis software with basic quantification tools to assess heart wall dynamics, more sophisticated processing and quantification tools are still required.

Quantitative analysis of intramyocardial layers seems well-suited to the well-known functional diversity of the subepicardial and subendocardial regions in different heart pathologies (Gallagher et al. 1982, 1985). Previous studies (Sabbah et al. 1981) proved that the subendocardium undergoes greater thickening and shortening than the epicardium; Sagar and colleagues found functional changes in the epi- and endocardium layers during ischaemia (Sagar et al. 1987). Myocardial gradient has been reported to be a good indicator of contractility defects in ischaemic segments (Garot et al. 1999; Pellerin et al. 1999). Other alternatives to evaluate myocardial contraction on M-mode grey-scale images have been explored, such as myocardial wall thickening and thinning (Guth et al. 1984; Jamal et al. 2001) obtained as the ratio between systole and diastole wall width.

One of the goals of quantitative analysis of complex dynamic studies is to generate simple indexes that are easier to interpret and to report than the whole set of images and curves. For this reason, it seems interesting to draw simple quantitative parameters from TDI information.

This paper presents a methodology and a software package developed to quantify M-mode TDI images, defining a number of quantitative parameters drawn from velocity and gradient curves obtained after segmenting the myocardial wall into anatomical layers.

The independent clinical predictive value of these parameters to detect motion abnormalities in the presence of ischaemia was evaluated in a comparative study between a group of healthy volunteers and patients with ischaemia.

MATERIALS AND METHODS

Image processing

According to a methodology previously described (Desco et al. 1996; Ledesma-Carbayo et al. 2000), the quantification procedure followed consists of:

1. Image acquisition of the M-mode TDI images;
2. colour decoding to extract the velocity values from colour TDI images;
3. image preprocessing (noise reduction and artefact removal);
4. definition of anatomical regions;
5. quantitative analysis.

These steps are described in detail in the following sections.

Image acquisition. Quantitative analysis of the TDI studies requires a meticulous protocol to acquire the images. Depending on the particular wall segment under study, the transducer position and M-mode scan line should be carefully located to scan perpendicularly the myocardial wall, avoiding subvalvular structures. Gain settings must assure a correct view of a conventional grey-scale image, with the focus placed in the myocardial wall. Doppler gain should be adjusted as to provide the largest span avoiding aliasing and artefacts from subvalvular structures. Some scanners allow mixing the grey-scale image with the colour TDI image, varying the transparency. This feature must be turned off to make sure that every colour in the image corresponds to only one velocity value, as required for a proper colour decoding. The acquisition of several cycles (two to five) is recommended to be able to reduce noise by cycle averaging.

Colour decoding. Most scanners used in cardiology export colour Doppler studies as true colour images with a colour overlay over a grey-scale image. Velocity information is coded through a colour table, usually displayed on the screen. Unfortunately, even standard image formats such as DICOM do not usually include the look-up table (LUT), which must be provided externally or calculated from the image itself by using the on-screen calibration bar. Special care should be taken when LUTs are nonlinearly compressed or expanded.

The effect of this nonlinearity on the accuracy of the quantification is difficult to assess. Analysis of images of a rotating phantom, as described in Fleming et al. (1994a), yields different degrees of accuracy depending on the particular colour table used. According to this, the use of strongly nonlinear LUTs should be disregarded, because the accuracy cannot be guaranteed and is not constant along the whole velocity span (Madrigal 2000; Santos et al. 2001).

Image preprocessing. Accuracy and precision have been characterised experimentally in TDI images using a rotating phantom (Santos et al. 2001) moving at a controlled velocity. The results showed two independent sources of error: a quasi-Gaussian (slightly leptokurtic distribution) noise with an SD of 2% of the velocity span and some artefacts or black spots, characterised as shot noise of higher amplitude.

The existence of these small black spots, which do not actually correspond to low velocities, is a very com-

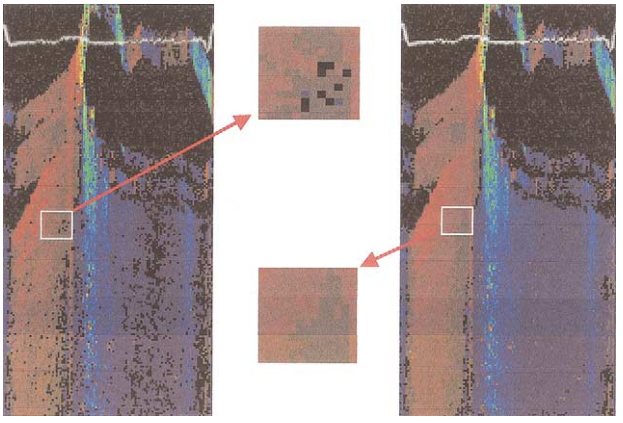

Fig. 1. Image enhancement obtained with the selective median filter (kernel size 11 × 11). Left = original image, right = filtered image. Zoomed regions are shown to better see the difference.

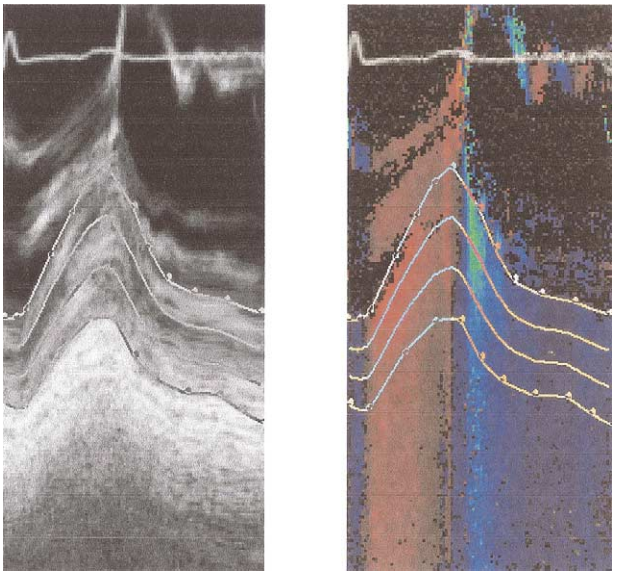

Fig. 2. Anatomical ROIs definition. Grey-scale image (left) is used to define the endocardial and epicardial limits. The cardiac wall is divided into three layers to be studied separately. Segmentation is exported to the TDI image (right).

mon artefact in TDI imaging. It degrades noticeably the quality of quantitative data and curves drawn from the images. To overcome this problem, we make use of a selective median filtering algorithm that fills these black spots without altering the remaining valid pixels.

Other authors have used median filtering for noise suppression in US images (Loupas et al. 1989). Our approach consisted in filtering only those pixels where the artefacts are present, and not modifying the signal level at other points. Artefacts are identified as those areas, of the appropriate size (1 to 4 mm, that translates into 2 to 8 pixels, depending on the spatial resolution used), where the difference between the original and the median-filtered images is higher than a threshold obtained from the random noise distribution as twice the SD (2σ). The procedure followed consists of 1. calculating a median filtered version of the original image with adjustable kernel size depending on spatial and temporal resolution, usually between 5×5 and 11×11 pixels; 2. computing the difference between the filtered version and the original image; 3. replacing by the filtered values all those points in the original image where the difference is higher than 2σ. Figure 1 shows an example of an image before and after applying the filter.

Another preprocessing step that can further improve signal-to-noise ratio (SNR) is the average of two or three cycles, provided the heart rate is regular and all the cycles show good quality. The procedure uses the ECG signal as a reference, and the averaging algorithm takes into account only those pixels with a velocity above a certain threshold; thus, avoiding the effect of possible residual black spots.

Definition of anatomical regions. Before performing the quantitative analysis, the cardiac wall is segmented into parallel layers. Some totally automatic methods have been proposed to define the myocardium borders either on grey-level images (Unser et al. 1989) or using combined TDI and grey-level data (Rabben et al. 2000). Because totally automatic methods are not fully reliable, our approach has been to develop an assisted interactive drawing tool that provides adequate reliability and repeatability for clinical studies. It allows for a fast and accurate identification of the cardiac wall borders with minimum user interaction, using spline interpolation (Unser 1999). Some scanners have the capability of providing both TDI and grey-scale images simultaneously; in this case, both images can be used to define the borders. Usually, wall limits are more easily identified on the grey-scale image, especially the epicardial border, as shown in Fig. 2.

After the endocardial and epicardial limits are defined, the wall is automatically divided into a number of parallel layers (usually three) of equal thickness.

Quantitative analysis. For each of the myocardial anatomical layers defined, mean velocity is calculated and plotted against time (Fig. 3).

The program also calculates the transmural velocity gradient, which represents the unitary spatial rate of velocity change across the wall:

$$\text{Velocity gradient} = \frac{-dW}{dt} \cdot \frac{1}{W}, \qquad (1)$$

where W represents wall thickness.

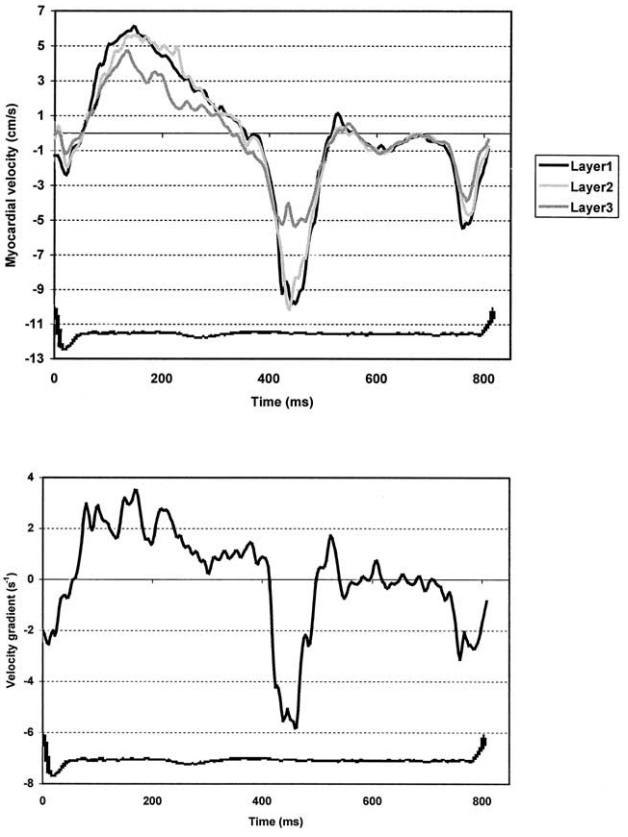

Fig. 3. Example of time curves from a healthy patient. Top, Velocity in the three layers; bottom, velocity gradient. The two diastolic components ("e" wave around 450 ms and "a" wave at 750 ms) can be clearly seen. ECG trace plotted at bottom.

Different approaches have been proposed to obtain this measurement. Fleming and colleagues (Fleming et al. 1994b) fitted a straight line to the velocity values, assuming a linear variation of the velocity across the myocardium.

In this work, we follow the approach proposed by Uematsu and colleagues (Uematsu et al. 1995) that simply uses the difference in myocardial velocity between endocardium and epicardium, divided by the myocardial wall thickness; this procedure also assumes linearity across the myocardium, to some extent.

$$\text{Velocity gradient} = (V_{endo} - V_{epi})/W, \qquad (2)$$

where V_{endo} and V_{epi} represent endocardium and epicardium velocities and W represents wall thickness.

From the velocity and gradient curves, several time- and amplitude-related parameters are automatically calculated, as detailed below (Fig. 4). They are grouped as "systole," "diastole" and "cycle" parameters.

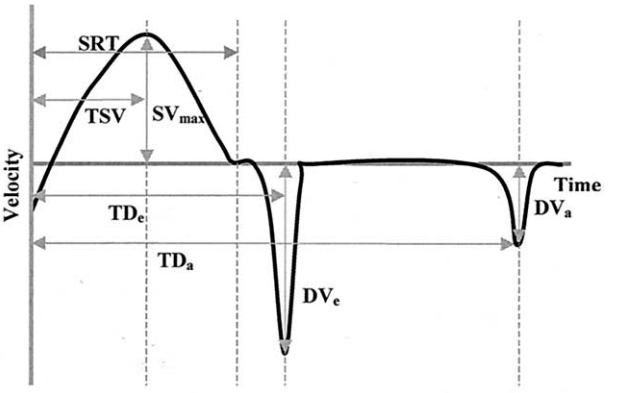

Fig. 4. Diagram of the proposed parameters in a model curve.

Systole parameters:

- Maximum and average curve values (SV_{max}, SV_{ave});
- Time from R wave to systole maximum (TSV);
- Systole relaxation time (SRT), defined as the time interval from the beginning of the cycle to the first zero-crossing after the systolic peak value. This parameter is only computed for the velocity curves.

Diastole parameters:

- Maximum values at early diastole (DV_e) and late diastole (DV_a), corresponding respectively to the "e" and "a" waves (see Fig 3);
- Time to early and late maxima (TD_e, TD_a).

Cycle parameters: these parameters are obtained by correlating the time curves with two periodic template functions; a pulse that models the ideal mechanical systole (spanning from the R-wave to the moment of maximum systolic contraction) and a sinusoid of frequency equal to the heart rate that represents the first harmonic of the signal.

- Two parameters are obtained from the cross correlation analysis with the pulse function: maximum cross correlation coefficient (CC) and time delay (TD), defined as the time shift at which maximum correlation is achieved.
- Amplitude (HA) and phase (HP) of the first harmonic, calculated by Fourier decomposition.

These parameters are similar to others previously proposed for integrated backscatter studies (Fitzgerald et al. 1987; Milunski et al. 1989; Sagar et al. 1987; Schecter et al. 1996).

Experimental setting

A validation protocol was designed to analyse if the different parameters obtained show significant changes in ischaemic patients and to determine which ones may show independent predictive value in the assessment of coronary heart disease.

TDI studies were obtained with a Siemens–Acuson® Sequoia scanner (Mountain View, CA) equipped with a phased-array 3.5-MHz and tissue Doppler imaging (TDI) protocol. Both colour TDI and grey-scale M-mode images were acquired and transferred to a PC in DICOM format. Images were analysed with an experimental software package that integrates all the procedures described above.

Data from the left ventricle basal posterior segment were acquired at rest from a parasternal long-axis view, according to the methodology described above. The study included 25 subjects grouped into two groups matched in age ranges: 17 healthy volunteers without any previous history of cardiovascular disease (age range 30 to 80 years old, 14 men) and 18 ischaemic patients (age range 30 to 79 years old, 4 men) with documented abnormal contractility (hipokinesia or akinesia) of basal posterior segments. Dis-synergy of this segment was assessed by stress echocardiography, evaluated by expert cardiologists. Scarring tissue was discarded, making sure that end-diastolic wall thickness was greater than 6 mm. Velocity and transmural gradient waveforms from three myocardial layers were obtained and analysed with the methodology proposed.

In this study, the ventricular wall was segmented into three layers, which roughly correspond to the endocardium, mesocardium and epicardium.

Statistical analysis

Univariate statistical analysis was performed on the basis of Student's *t*-tests, after checking normality of the data. No attempt to correct significance for multiple comparisons has been made because the strong association between many of the variables makes it difficult to estimate a proper number of degrees of freedom. Due to the high number of correlated variables, a reduction in dimensionality is advisable to identify a subset of reasonably independent parameters. To this end, a factorial analysis (principal components method with varimax rotation) was carried out on the variables that showed an individual significance better than $p < 0.05$. Finally, the joint predictive value of these parameters was assessed by means of stepwise logistic regression analysis. In all the multivariate procedures, model stability was carefully tested through jackknifing, randomly taking out 15% of the data in at least five different runs, always obtaining similar results. All the statistical procedures were performed with the SPSS version 10.0 (SPSS Inc., Chicago, IL) package.

RESULTS

Waveforms

An example of the velocity and gradient waveforms is presented in Fig. 3. A positive systolic lobe corresponding to the contraction wave is followed by a morphologically complex diastolic phase. An initial diastolic negative excursion follows the T wave of the ECG and the isovolumetric relaxation time, corresponding to the rapid filling period of the left ventricular cavity, after mitral valve opening. This first negative dominant wave of left ventricular relaxation coincides with the early wave (E wave) of the transmitral pulsed Doppler profile and, therefore, we designate it as diastolic "e" wave. A period without left ventricular wall motion follows, corresponding to diastasis. A second diastolic wave appears after the P wave of the ECG. This second wave is due to the late myocardial wall relaxation that follows mechanical contraction of left atrium. This contraction increases the pressure gradient between the left atrium and the left ventriculum, increasing the transmitral blood flow and forcing the myocardial wall to expand outwards during the late period of diastole. This late wave in the TDI curve is coincident with the A wave of the transmitral pulsed Doppler inflow and, therefore, we designate it as "a" wave.

Univariate analysis

From these curves, all the parameters described were obtained. Table 1 contains the results of the univariate statistical analysis, indicating the mean value and SD for each patient group (healthy and ischaemic) and the *p* value of each individual comparison. As can be observed, significance is clustered around gradient parameters (SV_{max}, SV_{ave}, DV_e, TD_a), and most systolic and diastolic layer velocity parameters are nonsignificant (except endocardium DV_e). Regarding cycle parameters, some values from cross-correlation and harmonic analysis show significant differences (mainly endocardium and epicardium CC and TD and HA of endocardium velocity and gradient).

Multivariate analysis

Results of the factorial analysis, intended to identify subsets of independent variables, are shown in Table 2. Three principal components were obtained: the first one includes the gradient variables (SV_e, HA, SV_{ave}, SV_{max}), the second one groups the CC parameter for the three layers and the third one includes the endo- and epicardial TD.

This analysis allowed us to select three variables for further processing, each one representative of each principal component: gradient SV_e, mesocardial CC and epicardial *TD*.

The stepwise logistic regression only introduced one variable with independent predictive value in the model: the gradient "e" wave maximum value (SV_e). With this only variable, the classification success rate reached 79.1% (sensitivity 82.6%, specificity 76.0%).

Table 1. Results from the analysis of 17 healthy and 18 patients with ischemia

		Endocardium velocity			Mesocardium velocity			Epicardium velocity			Gradient		
		Mean	(SD)	*p*	Mean	(SD)	*p*	Mean	(SD)	*p*	Mean	(SD)	*p*
SV_{max}	Ischemic	3.973	(1.694)	0.163	4.133	(1.618)	0.849	3.461	(1.537)	0.524	2.177	(1.722)	0.002*
	Normal	4.683	(1.192)		4.039	(1.216)		3.171	(1.074)		4.112	(1.683)	
SV_{ave}	Ischemic	1.811	(0.967)	0.372	1.849	(0.961)	0.764	1.540	(0.826)	0.118	0.347	(0.851)	0.000
	Normal	2.054	(0.547)		1.768	(0.566)		1.176	(0.450)		1.355	(0.587)	
TSV	Ischemic	0.176	(0.056)	0.270	0.210	(0.088)	0.552	0.173	(0.060)	0.512	0.229	(0.148)	0.325
	Normal	0.199	(0.063)		0.226	(0.073)		0.186	(0.057)		0.188	(0.087)	
SRT	Ischemic	0.446	(0.096)	0.555	0.437	(0.100)	0.515	0.423	(0.094)	0.651	–	–	–
	Normal	0.461	(0.052)		0.455	(0.054)		0.435	(0.054)		–	–	
DV_e	Ischemic	−6.171*	(3.289)*	0.008*	−5.307	(2.898)	0.068	−4.041	(1.945)	0.750	−3.854	(3.194)	0.002*
	Normal	−9.242*	(3.191)*		−7.106	(2.731)		−4.238	(1.651)		−7.831	(3.682)	
TD_e	Ischemic	0.551	(0.094)	0.241	0.550	(0.097)	0.274	0.542	(0.091)	0.221	0.559	(0.099)	0.390
	Normal	0.583	(0.063)		0.582	(0.069)		0.573	(0.051)		0.584	(0.064)	
DV_a	Ischemic	−3.436	(2.283)	0.233	−2.969	(1.996)	0.430	−2.328	(1.479)	0.818	−2.683	(2.291)	0.073
	Normal	−4.424	(2.531)		−3.511	(2.010)		−2.461	(1.893)		−4.011	(1.925)	
TD_a	Ischemic	0.943	(0.073)	0.253	0.944	(0.080)	0.197	0.933	(0.085)	0.369	0.963	(0.036)	0.016*
	Normal	0.916	(0.063)		0.913	(0.057)		0.910	(0.060)		0.919	(0.064)	
CC	Ischemic	0.774	(0.068)	0.001*	0.752	(0.068)	0.033*	0.761	(0.072)	0.005*	0.595	(0.179)	0.417
	Normal	0.712	(0.028)		0.711	(0.038)		0.691	(0.063)		0.636	(0.109)	
TD	Ischemic	−0.039	(0.041)	0.027*	−0.029	(0.048)	0.513	−0.023	(0.052)	0.016*	−0.105	(0.134)	0.072
	Normal	−0.010	(0.033)		−0.016	(0.063)		0.016	(0.035)		−0.042	(0.036)	
HA	Ischemic	1.097	(0.438)	0.012*	1.066	(0.492)	0.191	0.914	(0.463)	0.988	0.417	(0.222)	0.000*
	Normal	1.465	(0.377)		1.268	(0.396)		0.912	(0.319)		0.866	(0.377)	
HP	Ischemic	0.200	(0.083)	0.598	0.197	(0.079)	0.538	0.187	(0.080)	0.599	0.118	(0.268)	0.088
	Normal	0.212	(0.049)		0.211	(0.048)		0.199	(0.051)		0.235	(0.057)	

Parameter names are described in the text. Data show the mean value and SD in each group and the *p* value (Student's *t*-test). * Significant difference ($p < 0.05$). Units: SV_{max} SV_{ave} DV_e, DV_a, HA in cm/s (velocities) or s^{-1} (gradients); SRT, SRD, TD_e, TD_a, TD, HP are dimensionless (proportion relative to the RR period); CC dimensionless (correlation).

Forcing the other two variables in the model did not improve these rates.

All these results were consistently reproduced through the jackknifing process, where 15% of the cases were randomly eliminated in each run.

DISCUSSION

The univariate analysis found several significant parameters in the discrimination between healthy patients and those with ischaemia individually. It is well known that in normal subjects myocardial velocity is higher in endocardium than in the mesocardium or epicardium, resulting in a positive value of myocardial velocity gradient. This pattern changed in the patients with ischaemia, who showed a significantly lower velocity gradient. Comparing the two groups, mean and maximum systolic velocity gradients are significantly associated with the existence of ischaemia. Mean and peak systolic velocities, however, did not reach statistical significance. Accordingly, it seems that velocity values alone do not discriminate well between healthy patients and those with ischaemia.

Table 2. Results of factorial analysis: Rotated principal components

	Component		
Variable	1	2	3
Gradient SV_e	−0.909	0.080	−0.163
Gradient HA	0.882	−0.235	−0.079
Gradient SV_{ave}	0.801	−0.247	0.182
Gradient SV_{max}	0.794	−0.240	0.114
Endo SV_e	−0.700	0.007	−0.442
Gradient TA	−0.595	−0.290	−0.094
Endo HA	0.579	0.081	0.261
Epi CC	−0.089	0.930	−0.067
Meso CC	−0.115	0.925	−0.012
Endo CC	−0.020	0.880	−0.048
Epi TD	0.121	0.033	0.837
Endo TD	0.241	−0.167	0.777

The main finding of our study is that the maximum value of transmural gradient corresponding to the "e" wave (SV_e) seems the most adequate parameter to predict the existence of ischaemia. Multivariate analysis supports that the variables are structured into three main axis of variation, the cited parameter being the one that yields the best prognostic value regarding the existence of ischaemic disease. This seems an interesting finding because it allows reduction of the apparently high number of parameters that the proposed methodology produces.

On the other hand, it is interesting to try to explain why a diastolic parameter that measures the

gradient at the moment of the "e" wave resulted in being the most significant. Heart ischaemic disease is well known to impair diastolic myocardial wall motion of the left ventricle earlier than systolic contraction. Actually, the evaluation of left ventricle diastolic function has been largely used for the assessment of myocardial regions with reduced coronary perfusion (Bonow et al. 1985; Dawson and Gibson 1989; Garcia-Fernandez et al. 1999; Grossman 1990; Kondo et al. 1995; Ludbrook et al. 1981). It is interesting to remark that the "a" wave mostly depends on the atrial contraction, being less prone to show alterations in the transmural ventricular gradient than the "e" wave. Early diastolic relaxation is known to be an active phenomenon that takes place at higher energy expenditure than passive late diastolic motion. This may constitute the physiologic basis underlying our findings of a low "e" wave velocity as the most sensitive sign of hypoperfusion. This observation of an altered diastolic "e" wave in ischaemic left ventricular wall segments is also in agreement with previous experimental studies with pulsed-wave Doppler imaging (Garcia-Fernandez et al. 1999), observing decreased peak early diastolic velocity of the myocardial wall.

Recently, Derumeaux and colleagues analysed the utility of TDI to quantify the variation of endocardial and epicardial velocities during ischaemia in an experimental model (Derumeaux et al. 2000). They showed that ischemia caused a significant and comparable reduction in endocardial and epicardial systolic velocities in the anterior wall with the disappearance of the velocity gradient. Our results mostly confirm their findings, having detected this reduction in endocardial systolic velocities and systolic velocity gradient in ischemia, although we did not find the same reduction in epicardium. This may be in relation with the severity of the ischemia (transmural or not transmural ischemia or infarct).

Cycle parameters, intended to assess the phase of the velocity curves, were not good predictive variables and most of them did not even reach significance in the univariate analysis. Our implementation of these measurements roughly followed the ones that previously had reported good results using integrated backscatter curves (Fitzgerald et al. 1987; Milunski et al. 1989; Sagar et al. 1987; Schecter et al. 1996). These parameters do not seem optimal for the purpose of detecting ischaemia with TDI. A possible explanation may lie in the different shape of the curves obtained from integrated backscatter, which are smoother and show a more regular pattern within the cycle.

In this study, echocardiograms were only performed at rest. Although ischaemia is better diagnosed with stress echocardiography, it has also been detected at rest (Ghali et al. 1991; Perrone et al. 1991). If the quantitative procedure proposed combined with stress interventions could improve diagnostic accuracy remains to be determined.

The high classification rates obtained must be carefully interpreted, as they regard the same data set used to calculate the logistic regression. Future validation of these figures on independent data sets is required.

Limitations of our clinical study are the possibly imperfect matching between groups and the low number of cases studied. This number, however, has proven to be enough to assess the significance of the individual parameters, and to construct a stable multivariate model. Nevertheless, new independent studies recruiting more patients could confirm our results, also contributing to define cut-off values for the parameters.

Another limitation is that we have restricted the analysis to a single segment in the posterior wall, since velocity obtained from M-mode images is only accurate when the ultrasound beam is perpendicular to the myocardium. The basal segment of the posterior wall is the one that best fulfills this condition. We have also restricted the analysis to a single pathology (ischaemic heart disease). It could be conceivable that for other pathologies or segments, other parameters might result more adequate than the ones described here.

The preprocessing techniques applied showed to be very useful in fixing up non-optimum studies. However, as with any echocardiographic technique, a very low quality echo image limits the possibility of obtaining quantitative assessment of ischaemic left ventricular segments in patients with coronary artery disease.

The study of the ventricular wall segmented in three layers that roughly correspond to the endocardium, mesocardium and epicardium, seems appropriate, although a division in more layers, intended to allow for finer relative stress measurements, has been proposed (Marcos-Alberca et al. 2001).

CONCLUSIONS

The software package developed can be used in a clinical environment, providing objective measurements. The proposed methodology provides parameters that allow discrimination between healthy and abnormal myocardial tissue. The statistical analysis performed has proved that any single parameter related to the gradient intensity, particularly the maximum gradient at the moment of the "e" wave, provides meaningful clinical information. Adding additional parameters does not improve the diagnostic performance. The rate of correct classification reached 79.1% (sensitivity 82.6%, specificity 76.0%) on the same data set used for the analysis.

Further studies using modifications of the technique (other pathologies, different views, pharmacological or stress interventions, etc.) are warranted.

Acknowledgements—This work has been partially supported by grants from Comunidad de Madrid (III-PRICYT), Fondo de Investigaciones Sanitarias (00/0036), CICYT (99/1085-C02) and also with funds from a research contract with Acuson (A Siemens Company).

REFERENCES

Bonow RO, Vitale DF, Bacharach SL, et al. Asynchronous left ventricular regional function and impaired global diastolic filling in patients with coronary artery disease: Reversal after coronary angioplasty. Circulation 1985;71:297–307.

Dawson JR, Gibson DG. Left ventricular filling and early diastolic function at rest and during angina in patients with coronary artery disease. Br Heart J 1989;61:248–257.

Derumeaux G, Cochonneau O, Douillet R, Cribier A, Letac B. Comparison of myocardial velocities by tissue color Doppler imaging in normal subjects and in dilated cardiomyopathy. Arch Mal Coeur Vaiss 1997;90:773–778.

Derumeaux G, Ovize M, Loufoua J, et al. Doppler tissue imaging quantitates regional wall motion during myocardial ischemia and reperfusion. Circulation 1998;97:1970–1977.

Derumeaux G, Ovize M, Loufoua J, et al. Assessment of nonuniformity of transmural myocardial velocities by color-coded tissue Doppler imaging: Characterization of normal, ischemic, and stunned myocardium. Circulation 2000;101:1390–1395.

Desco M, Antoranz JC. Technical principles of Doppler tissue imaging. In: García-Fernández MA, Zamorano JL, Azevedo J, eds. Technical principles of Doppler tissue imaging. New York: McGraw-Hill, 1997.

Desco M, Antoranz C, García-Fernández MA. Quantitative analysis of colour-coded Doppler tissue images. In: Lemke HU, Inamura K, Farman AG, eds. Computer assisted radiology CAR'96. Amsterdam: Elsevier Science, 1996:1004.

Donovan CL, Armstrong WF, Bach DS. Quantitative Doppler tissue imaging of the left ventricular myocardium: Validation in normal subjects. Am Heart J 1995;130:100–104.

Fitzgerald PJ, McDaniel MD, Rolett EL, Strohbehn JW, James DH. Two-dimensional ultrasonic tissue characterization: Backscatter power, endocardial wall motion, and their phase relationship for normal, ischemic, and infarcted myocardium. Circulation 1987;76:850–859.

Fleming AD, McDicken WN, Sutherland GR, Hoskins PR. Assessment of colour Doppler tissue imaging using test-phantoms. Ultrasound Med Biol 1994a;20:937–951.

Fleming AD, Xia X, McDicken WN, Sutherland GR, Fenn L. Myocardial velocity gradients detected by Doppler imaging. Br J Radiol 1994b;67:679–688.

Gallagher KP, Osakada G, Hess OM, et al. Subepicardial segmental function during coronary stenosis and the role of myocardial fiber orientation. Circ Res 1982;50:352–359.

Gallagher KP, Stirling MC, Choy M, et al. Dissociation between epicardial and transmural function during acute myocardial ischemia. Circulation 1985;71:1279–1291.

Garcia-Fernandez MA, Azevedo J, Moreno M, et al. Regional diastolic function in ischaemic heart disease using pulsed wave Doppler tissue imaging. Eur Heart J 1999;20:496–505.

García-Fernández MA, Zamorano JL, Azevedo J. Doppler tissue imaging. New York: McGraw-Hill, 1997.

Garot J, Derumeaux GA, Monin JL, et al. Quantitative systolic and diastolic transmyocardial velocity gradients assessed by M-mode colour Doppler tissue imaging as reliable indicators of regional left ventricular function after acute myocardial infarction. Eur Heart J 1999;20:593–603.

Garot J, Diebold B, Derumeaux G, Gueret P. Alterations of left ventricular mechanics after anterior myocardial infarction. Quantitative analysis by tissue Doppler echocardiography. Arch Mal Coeur Vaiss 2000;93:1211–1220.

Ghali JK, Kadakia S, Cooper RS, Liao YL. Bedside diagnosis of preserved versus impaired left ventricular systolic function in heart failure. Am J Cardiol 1991;67:1002–1006.

Gorcsan J III, Strum DP, Mandarino WA, Gulati VK, Pinsky MR. Quantitative assessment of alterations in regional left ventricular contractility with color-coded tissue Doppler echocardiography. Comparison with sonomicrometry and pressure-volume relations. Circulation 1997;95:2423–2433.

Grossman W. Diastolic function and heart failure: An overview. Eur Heart J 1990;11(Suppl. C):2–7.

Guth B, Savage R, White F, et al. Detection of ischemic wall dysfunction: Comparison between M-mode echocardiography and sonomicrometry. Am Heart J 1984;107:449–457.

Jacob G, Noble JA, Mulet-Parada M, Blake A. Evaluating a robust contour tracker on echocardiographic sequences. Medi Image Anal 1999;3:63–76.

Jamal F, Szilard M, Kukulski T, et al. Changes in systolic and postsystolic wall thickening during acute coronary occlusion and reperfusion in closed-chest pigs: Implications for the assessment of regional myocardial function. J Am Soc Echocardiogr 2001;14:691–697.

Kondo H, Masuyama T, Ishihara K, et al. Digital subtraction high-frame-rate echocardiography in detecting delayed onset of regional left ventricular relaxation in ischemic heart disease. Circulation 1995;91:304–312.

Ledesma-Carbayo M, Malpica N, Desco M, et al. Quantitative intramyocardial M-Mode DTI analysis. In: S Loncaric Ed. Proceedings of IWISPA 2000. Pula, Croatia, 2000:133–138.

Loupas T, McDiccken WN, Allan PL. An adaptive weighted median filter for speckle suppresion in medical ultrasonic images. IEEE Trans Circ Syst Vid 1989;36:129–135.

Ludbrook PA, Byrne JD, Tiefenbrunn AJ. Association of asynchronous protodiastolic segmental wall motion with impaired left ventricular relaxation. Circulation 1981;64:1201–1211.

Madrigal M. Diseño de fantomas para ecocardiografía Doppler. MA thesis. Madrid: Universidad Politécnica de Madrid, 2000:230.

Malassiotis S, Strintzis MG. Tracking the left ventricle in echocardiographic images by learning heart dynamics. IEEE Trans Med Imaging 1999;18:282–291.

Marcos-Alberca P, García-Fernández MA, Desco M, et al. Intramyocardial analysis of regional systolic and diastolic function in ischemic heart disease with Doppler tissue imaging: Role of the different myocardial layers. J Am Soc Echocardiogr 2002;15:99–108.

Milunski MR, Mohr GA, Wear KA, et al. Early identification with ultrasonic integrated backscatter of viable but stunned myocardium in dogs. J Am Coll Cardiol 1989;14:462–471.

Miyatake K, Yamagishi M, Tanaka N, et al. New method for evaluating left ventricular wall motion by color-coded tissue Doppler imaging: In vitro and in vivo studies. J Am Coll Cardiol 1995;25:717–724.

Palka P, Lange A, Fleming AD, et al. Doppler tissue imaging: Myocardial wall motion velocities in normal subjects. J Am Soc Echocardiogr 1995;8:659–668.

Pellerin D, Berdeaux A, Cohen L, et al. Comparison of 2 myocardial velocity gradient assessment methods during dobutamine infusion with Doppler myocardial imaging. J Am Soc Echocardiogr 1999;12:22–31.

Perrone F, Bacharach S, Dilsizian V, Bonow R. Impaired left ventricular filling and regional diastolic asynchrony at rest in coronary artery disease and relation to exercise-induced myocardial ischaemia. Am J Cardiol 1991;67:356–360.

Rabben SI, Torp AH, Stoylen A, et al. Semiautomatic contour detection in ultrasound M-mode images. Ultrasound Med Biol 2000;26:287–296.

Sabbah HN, Marzilli M, Stein PD. The relative role of subendocardium and subepicardium in left ventricular mechanics. Am J Physiol 1981;240:H920–H926.

Sagar KB, Rhyne Tl, Warltier DC, Pelc L, Wann LS. Intramyocardial variability in integrated backscatter: Effects of coronary occlusion and reperfusion. Circulation 1987;75:436–442.

Santos A, Ledesma-Carbayo MJ, Malpica N, et al. Accuracy of heart strain rate calculation derived from Doppler tissue velocity data. In:

Insana MF, Shug KK, eds. Proceedings of the SPIE Medical Imaging Symposium, 2001. San Diego, 2001:546–556.
Schecter SO, Teichholz LE, Klig V, Goldman ME. Ultrasonic tissue characterization: Review of a noninvasive technique for assessing myocardial viability. Echocardiography 1996;13:415–430.
Sutherland GR, Stewart MJ, Groundstroem KW, et al. Color Doppler myocardial imaging: A new technique for the assessment of myocardial function. J Am Soc Echocardiogr 1994;7:441–458.
Uematsu M, Miyatake K, Tanaka N, et al. Myocardial velocity gradient as a new indicator of regional left ventricular contraction: Detection by a two-dimensional tissue Doppler imaging technique. J Am Coll Cardiol 1995;26:217–223.
Unser M. Splines. A perfect fit for signal and image processing. IEEE Signal Process Magazine 1999;16(6):22–38.
Unser M, Pelle G, Brun P, Eden M. Automatic extraction of serial myocardial borders from M-mode echocardiograms. IEEE Trans Med Imaging 1989;8:96–103.
Yamazaki N, Mine Y, Sano A. Analysis of ventricular wall motion using colour-coded tissue Doppler imaging system. Jpn J Appl Phys 1994;33:3141–3146.